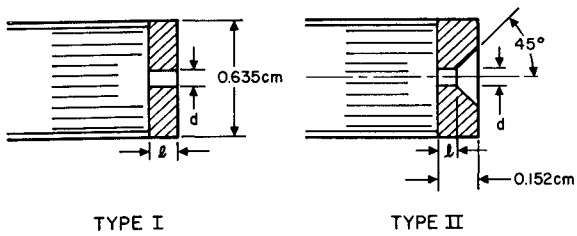

Fig. 6 Hollow cathode tip and orifice configurations.

At the outset of the program a hollow cathode configuration was required which could operate at 10-amp emission without severe erosion of the orifice. The initial design was of type I shown in Fig. 6 with $d = 0.038$ cm and $l = 0.152$ cm. It eroded rapidly during the first few hours of operation, after which the erosion rate reduced. Drawing on the results of Rawlin and Kerslake[4] and testing cathodes with variations in d and l, it was determined that initial erosion was proportional to the self-heated operating temperature, which increases with increasing l or decreasing d. Since the initial erosion usually has the form of a chamfering of the orifice, configuration II of Fig. 6 was chosen. It permits a short l without severely impairing the thermal conduction of heat from the orifice region (which always appears brighter than the rest of the cathode tip when viewed with a pyrometer). The values of l and d which displayed no initial erosion were $l = 0.051$ cm and $d = 0.076$.

Evaluation Testing

The 500-hr test was continuously manned, and data were recorded at half-hour intervals. A data summary is presented in Table 3. All components except the dielectric-coated accelerator grid performed extremely well. The plasma bridge neutralizer operated well with no indication of a change in its properties. The propellant electrical isolators showed no increase in leakage throughout the 500 hr. No erosion could be detected on the thruster hollow cathode orifice. Three accelerator grids had to be used to complete the 500-hr test period. The failure mode cannot be, at present, convincingly explained. Several investigations are under way to determine whether the failure problem is basic in nature, or the result of inadequate technological development in either the fabrication or testing procedures.

Table 3 500-hr test performance summary

Parameter	Total test[a] V, v	I, amp	P, w
Beam	1000	1.854	1854.0
Discharge	40.9	8.6	353.0
Accelerator[b]	405	0.050	70.2
Cathode and isolator heater	18.1	2.8	50.6
Neutralizer heater	5.0	2.9	14.5
Cathode keeper	8.0	0.28	2.2
Neutralizer keeper	9.7	0.22	2.1
Main vaporizer	3.6	2.4	8.6
Cathode vaporizer	2.3	2.0	4.6
Neutralizer vaporizer	1.5	1.1	1.6
Neutralizer coupling[c]	21.9	1.854	40.6
Total power		2,402.0 w	
Total losses		548.0 w	
Electrical efficiency		77.1%	
Mass efficiency		90.0%	
Total efficiency		69.4%	
Thrust		27.0 mlb	
I_{sp}		2,846 sec	
Power/thrust		89 w/mlb	
ev/ion		190	
Main flow rate		1.02 cm³/hr	
Cathode flow rate		0.077 cm³/hr	
Neutralizer flow rate		0.042 cm³/hr	

[a] Test conducted in three segments using different ion optical systems.
[b] Accel power is computed as $I_{accel} \times V_{total}$.
[c] Neut. coupling volt = thruster floating potential plus estimated beam potential of 12 v.

Conclusions

An engineering model of a 30-cm-diam thruster module has been developed for operation at 2-½-kw power level and I_{sp} of 2850 sec. Extensive testing has shown it to possess the performance characteristics suitable for a solar-electric-propulsion, deep-space mission. The performance characteristics here should represent state-of-the-art for a thruster module of this size.

References

[1] King, H. J., Poeschel, R. L., and Ward, J. W., "A 30 cm, Low Specific Impulse, Hollow Cathode Mercury Thruster," *Journal of Spacecraft and Rockets*, Vol. 7, No. 4, April 1970, pp. 416–421.

[2] Bechtel, R. T., "Performance and Control of a 30 cm Diameter Low Impulse Kaufman Thruster," *Journal of Spacecraft and Rockets*, Vol. 7, No. 1, Jan. 1970, pp. 21–25.

[3] King, H. J. and Poeschel, R. L., "Low Specific Impulse Ion Engine," CR 72677, 1970, NASA.

[4] Rawlin, V. K. and Kerslake, W., "Durability of the SERT II Hollow Cathode and Future Applications of Hollow Cathodes," *Journal of Spacecraft and Rockets*, Vol. 7, No. 1, Jan. 1970, pp. 14–20; also TMX 52532, 1969, NASA.

Ground and Flight Test Results for a Decelerator Towline Energy Absorber

Ross L. Goble* and Earl L. Councill Jr.†
NASA Langley Research Center, Hampton, Va.

EARLY flights in the Planetary Entry Parachute Program (PEPP) indicated a high shock peak and an oscillatory response of the payload during early phases of payload deceleration.[1,2] The oscillations appeared to be more severe at increased Mach numbers. Since an even higher Mach number ($M = 3.5$) was planned for the disk-gap-band parachute (Fig. 1) in the Supersonic High Altitude Planetary Experiment (SHAPE) program, it appeared that shock attenuation would be required. This Note presents the experimental effort associated with the design of the energy

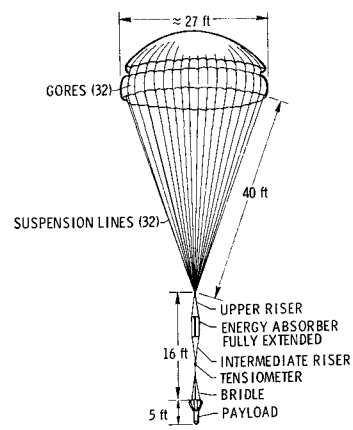

Fig. 1 Parachute dimensional details and flight configuration.

Presented as Paper 70-1202 at the AIAA Aerodynamic Deceleration Systems Conference, September 14–16, Dayton, Ohio; submitted October 8, 1970; revision received December 16, 1970.

* Aero-Space Technologist. Member AIAA.
† Aero-Space Technologist.

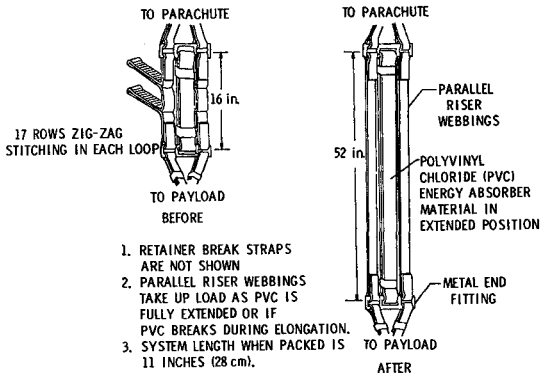

Fig. 2 Conceptual design of energy absorber.

absorber used in the SHAPE Mach 3.3 flight.[3] Because the payload canister was already designed at the inception of the absorber design phase, physical size limitations imposed by the available canister space were very important in the choice of the absorber design.

Energy Absorber Experiments

One requirement was that the absorber should have good attenuation capability over a rather long stroke consistent with the initial length prescribed by the canister size constraints. For this reason, a highly plasticized polyvinyl chloride (PVC) flat tape, which had proved successful for subsonic parachute shock attenuation,[4] was used. In addition, dacron break straps and webbing with pull-out

Table 1 PVC pull-test results

Specimen gage length, in.	Test no.	Force at break, lb	Length at break, in.	Remarks
6	1E	42.3	19.2	Pulled 20 in./min to break point
	1F	41.5	18.3	Cycled five imes after 12 in. Δl, then taken to break point
	1G, L	43	19.9	Broke at upper jaw
	1H, I, K	43	19.9–20.0	Broke at lower jaw
	1J	40.5	18.8	
	7, 9	275	19.9	Broke 1 of 6 plies
	8	270	19.6	Broke 2 of 6 plies
2	10–15	50–52	6.7–7.5	Broke at upper jaw
5½*	3D	96	15.8 (Broke 2 plies)	*Distance between D rings (to examine D ring radius effect)
	4D	86	14.6	Heat-sealed joint

stitchery were employed to enhance operational characteristics of the absorber (Fig. 2). Three preflight test sequences were as follows:

1) Pull tests of the tape were made with sample gage lengths (initial unstretched length between the Instron tester's jaws) of 4 and 8 in. A maximum travel of 20 in./min was used, yielding strain rates of 5 and 2.5 in./in.-min for the two lengths, respectively. Attempts to impose a higher strain rate by using 1-in.-gage-length specimens gave non-

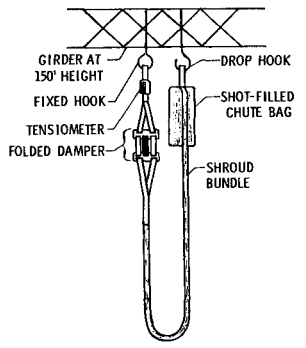

Fig. 3 Schematic of drop test.

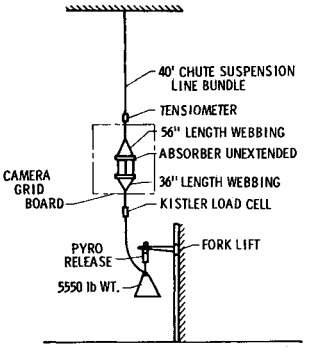

Fig. 4 Constant load drop-test elements.

repeatable results, because end effects became quite significant. Dacron break straps and webbing stitchery were qualified through static load tests.

2) Two types of drop-loading tests were performed on the shroud line system. To simulate opening shock, a parachute bag filled with lead shot (Fig. 3) was used to induce a 5000-lb shock load. After obtaining the transient loading spike by means of load cell and high-speed oscillograph, tests on the shroud system were made with and without the absorber installed. The second drop-test setup (Fig. 4) simulated also the sustained aerodynamic load subsequent to opening shock. High response instrumentation recorded the load response as measured by a tensiometer and a load washer. The initial load was varied by changing the vertical position of the fork lift.

Table 2 Dacron break strap and stitched webbing test results

Specimen	Test no.	Force at break, lb	Remarks
Dacron strap	2	2580	Single strap, static load
	4–6	2420	Single strap, static load
Stitched web	1–3	600–630	lb per row of stitching

3) The extraction mode of the final absorber configuration was tested with a cross-type parachute[5] in two low-altitude drops from helicopters.

Results of Ground and Flight Tests

The pull tests of the PVC tape (Table 1) showed that the ratio of break length to original unstretched length (~3) is reasonably repeatable. For the imposed strain rates of 5 and 2.5 in./in.-min, no strain-rate sensitivity effects on elongation at failure were noted. A force-deflection curve integrator was employed on cyclic pull tests to confirm the energy absorption characteristics of the PVC, and the results were used to establish the flight energy absorber design. Data obtained for the dacron break straps and the stitched webbing are presented in Table 2.

In the first drop-test series some nonrepeatability of data was noted and was due primarily to sporadic lateral wind deflection of the suspended (Fig. 3) test item. Results of the rebound characteristics for damped and undamped motion

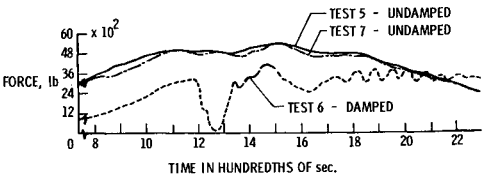

Fig. 5 Drop-test force time histories.

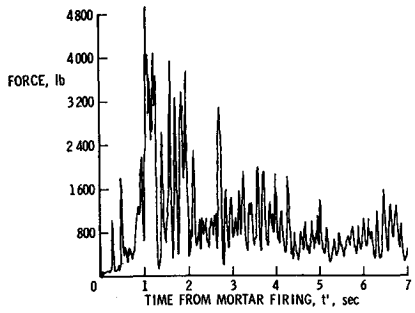

Fig. 6 Time history of force measured by the tensiometer.

for a calm day employing excursions measured directly from high-speed motion-picture film are compared in Table 3, and Fig. 5 shows the transient load curves for the same three tests. In the second drop-test series (Fig. 4), an opening shock load of 6230–6300 lb was followed by a sustained load of 5550 lb. All elements of the damper were fully elongated without failure.

Two sets of a flight-type energy absorber hardware (Fig. 2) were then taken to El Centro, Calif. for low-altitude drop tests. The damper bundle of each flight article comprised 53 layers of PVC film with a total thickness of 0.45 in. (1.14 cm). Two break straps of dacron (not shown in Fig. 2) restrained the PVC from opening until the onset of the initial maximum canopy inflation. The primary objective of demonstrating extraction of the absorber from its small-clearance fit in the payload canister without damage was accomplished in both tests, but these low-altitude drops from helicopters were nonrepeatable with regard to opening shock level, such that attenuation capability relative to the undamped system could not be determined. Examination of the recovered absorbers indicated that interlayer friction caused fusing of the PVC layers in the damper bundle during operation. Therefore, one change made for supersonic flight test items was the use of talcum powder sprinkled between the PVC layers.

In the Mach 3.3 flight at the White Sands Missile Range, New Mexico, all elements of the energy absorber performed their designed functions. The initial load peak at 1.03 sec after mortar firing (Fig. 6) produced a 21.1-g deceleration and was associated with the breaking of the aforementioned dacron break straps. Subsequent loads did not exceed the ~15-g deceleration load for which the absorber had been designed. Other occurrences during the mission, however, preclude complete assessment of the absorber effectiveness. Details of the canopy damage which is believed to have been caused by aerodynamic heating and which could have also have a load-alleviating effect are given in Ref. 3. Response characteristics for a Mach 2.7 flight without the attenuator are compared with those for the Mach 3.3 flight with the attenuator in Fig. 7. Although higher loads would have been anticipated for the latter flight based on extrapolation of earlier undamped flight data, it can be seen that the load levels were considerably reduced.

Concluding Remarks

It is felt that the absorber appreciably reduced the severity of the payload response to parachute opening shock loads,

Table 3 Load amplitude data—drop series I

Test no.	Configuration	Load at first rebound, lb	Drop distance, ft	Rebound height, ft
5, 7	Undamped	5000, 4950	55	22.5
6	Damped	2720	55	10.6

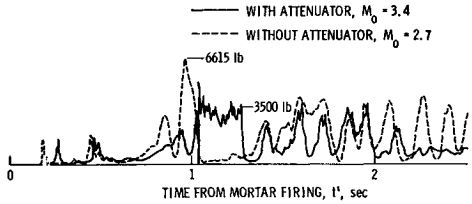

Fig. 7 Flight tensiometer records.

and that better stroke and absorption characteristics could be obtained if the design were not limited by volumetric constraints. It is recommended that consideration be given to the development of lightweight, long-stroke energy absorption devices.

References

[1] Preisser, J. S. and Eckstrom, C. V., "Flight Test of a 40-Foot-Nominal-Diameter Disk-Gap-Band Parachute Deployed at a Mach Number of 1.91 and a Dynamic Pressure of 11.6 Pounds Per Square Foot," TM X-1575, 1968, NASA.

[2] Eckstrom, C. V. and Preisser, J. S., "Flight Test of a 40-Foot-Nominal-Diameter Disk-Gap-Band Parachute Deployed at a Mach Number of 2.72 and a Dynamic Pressure of 9.7 Pounds Per Square Foot," TM X-1623, 1968, NASA.

[3] Eckstrom, C. V., "Flight Test of a 40-Foot-Nominal-Diameter Disk-Gap-Band Parachute Deployed at a Mach Number of 3.31 and a Dynamic Pressure of 10.6 Pounds Per Square Foot," TM X-1924, 1970, NASA.

[4] Gray, J. H., "Attenuation of Deployment and Opening Forces of Certain Aerodynamic Decelerators," *Proceedings—Symposium on Parachute Technology and Evaluation*, Vol. II, edited by Earl C. Myers, FTC-TDR-64-12, U.S. Air Force, 1964, pp. 502–508.

[5] Preisser, J. S. and Eckstrom, C. V., "Flight Test of a 30-Foot-Nominal-Diameter Cross Parachute Deployed at a Mach Number of 1.57 and a Dynamic Pressure of 9.7 Pounds Per Square Foot," TM X-1542, 1968, NASA.

A Shielded Fine-Wire Probe for Rapid Measurement of Total Temperature in High-Speed Flows

LEONARD M. WEINSTEIN*
NASA Langley Research Center, Hampton, Va.

Nomenclature

A ≡ parameter defined as $(k_0/k)^{1/2}Nu^{1/2}L/D$
d = probe height, in.
K_d = Knudsen number, $(= 1.26\gamma^{1/2}M_\infty/Re_{\infty,d})$
k = thermal conductivity of wire material
k_0 = thermal conductivity of gas evaluated at the gas total temperature
M = Mach number
p = pressure
$Re_{\infty,d}$ = Reynolds number $\rho_\infty u_\infty d/\mu_\infty$
Re_i, Re_0 = $\rho_i u_i d/\mu_{t,\infty}$ and $\rho_\infty u_\infty d/\mu_{t\infty}$, respectively
L/D = length diameter ratio of sensing wire
Nu = Nusselt number
R_w = resistance of wire, ohms
T = temperature, °R
u = gas velocity, fps
γ = ratio of specific heats
ξ = $(T_t - T_w)/(T_t - T_s)$
Φ = $\xi/(1-\xi) = (T_t - T_w)/(T_w - T_s)$
ρ,μ = density and viscosity, respectively

Received November 2, 1970; revision received December 21, 1970.

* Aerospace Engineer, Aero-Physics Division.